MOEM

Modern Electronic Materials 2024; 10(4): 243–250
DOI 10.3897/j.moem.10.4.140641

Research Article

Dynamics of monoatomic steps on the Si(100) surface during MBE growth and post-growth annealing

Yuri Yu. Hervieu[1], Michael Yu. Yesin[2], Alexander S. Deryabin[2], Alexey V. Kolesnikov[2], Alexander I. Nikiforov[2]

1 National Research Tomsk State University, 36 Lenin Ave., Tomsk 634050, Russian Federation

2 Rzhanov Institute of Semiconductor Physics, Siberian Branch of the Russian Academy of Sciences, 13 Lavrentiev Ave., Novosibirsk 630090, Russian Federation

Corresponding author: Yuri Yu. Hervieu (ervye@mail.tsu.ru)

Received 29 September 2024 ♦ **Accepted** 28 November 2024 ♦ **Published** 30 December 2024

Citation: Hervieu YuYu, Yesin MYu, Deryabin AS, Kolesnikov AV, Nikiforov AI (2024) Dynamics of monoatomic steps on the Si(100) surface during MBE growth and post-growth annealing. *Modern Electronic Materials* 10(4): 243–250. https://doi.org/10.3897/j.moem.10.4.140641

Abstract

The dynamics of monoatomic steps on the Si(100) vicinal surface during molecular beam epitaxy (MBE) growth and annealing is studied based on the analysis of reflection high-energy electron diffraction intensity variations. During growth, the initially equally spaced A- and B-steps are getting closer: the width of the A-terraces decreases to a certain minimum value, which increases with increasing growth temperature. The number of Si monolayers deposited until the minimum distance between the A- and B steps is reached increases monotonically with increasing temperature.

After interrupting the Si deposition flux (during annealing) the width of the A-terrace gradually increases to the initial value. The time of such relaxation to the initial configuration of the steps decreases with increasing temperature and increasing miscut angle. The observed behavior of the steps during annealing is in good agreement with the available theoretical models of the step dynamics and is explained by the presence of an exchange flux of Si atoms between the A- and B-steps due to the elastic interaction of the steps caused by the anisotropy of the elastic stress tensor on the reconstructed Si(100) surface. However, the available models fail to explain the experimentally observed monotonically increasing temperature dependence of the number of Si monolayers deposited until the steps approach each other during growth, which indicates the need to modify the model of incorporation of Si adatoms into steps in the case of high temperatures.

Keywords

molecular beam epitaxy, diffraction, Si(100) surface, terraces, steps, kinks, adatoms

1. Introduction

The Si(100) surface is the base surface for the formation of various semiconductor nanostructures as well as a prototypical system for studying the features of epitaxial growth on reconstructed surfaces [1, 2]. As is known, on the reconstructed 2×1 Si(100) surface deviated from the (100) plane to the (111) plane by a certain angle θ (the vicinal surface Si(100)-2×1) elementary steps of different types can be present: monoatomic A- and B-steps and bi-atomic (double) D_A and D_B steps. The presence of mono-atomic vicinal steps prevents the formation of high-quality epitaxial films of III–V compounds on Si(100) substrates

© 2024 National University of Science and Technology MISIS. This is an open access article distributed under the terms of the Creative Commons Attribution License (CC-BY 4.0), which permits unrestricted use, distribution, and reproduction in any medium, provided the original author and source are credited.

due to the generation of interphase boundaries [3]. For this reason, for heteroepitaxy of III–V compounds on silicon the substrates with relatively large miscut angles (θ > 2°) are used, at which, according to the thermodynamic calculations [4], biatomic steps should form (the so-called single-domain surface Si(100)-2×1). However, in practice, Si(100) substrates with small miscut angles of up to 0.5° are most widely used. Therefore, searching the conditions under which the formation of single-domain vicinal Si(100) surfaces at small miscut angles is possible is highly demanded.

In this regard, it is important that reflection high-energy electron diffraction (RHEED) and scanning tunneling microscopy (STM) studies have shown the possibility of forming a single-domain surface under nonequilibrium conditions at the miscut angles smaller than those predicted by thermodynamic calculations [6–10]. Thus, STM studies have demonstrated a rapid (in a time shorter than the growth time of a silicon monolayer) formation of biatomic steps during Si deposition on the substrate with a miscut angle of 0.5° [6, 7]. The rapid formation of the single-domain surface during growth was observed with RHEED by Sakamoto et al. [8]. These authors also demonstrated gradual recovery of the two-domain surface structure after interruption of the Si flux (i.e. during post-growth annealing).

The available models of step motion on the Si(100) surface associate the transition to a single-domain surface during growth to the hindered incorporation of adatoms into the A-step. During growth, the edge of the fast moving B-step gets closer to the edge of the slow moving A-step until some minimum width of the A-terrace is reached, after which the steps move with equal velocities. In the Stoyanov's model [11], the hindered incorporation of adatoms into the A-step is due to a lower concentration of kinks on the smooth edge of the A-step as compared to the rough edge of the B-step. In the model [12], the presence of conventional and inverse Ehrlich–Schwoebel barriers [13, 14] for the attachment of adatoms to the A-step is assumed, due to which almost all atoms arriving at the surface from the molecular beam incorporate into the B-steps. In [15], it was shown that rapid formation of biatomic steps is possible even in the absence of the conventional Ehrlich–Schwoebel barrier, if adatoms are able to cross the A-step before being incorporated into the kinks on the step (the so-called permeable A-step [16, 17]). It is important that the models [12, 15] take into account the elastic interaction between the steps, which arises mainly due to the anisotropy of the stress tensor on the reconstructed Si(100) surface [4]. This makes it possible to explain the increase in the steady-state (or minimum) width of the A-terrace with increasing temperature and decreasing growth rate [10, 12].

It should be noted that the models [12, 15], with an appropriate choice of parameters, demonstrate good quantitative agreement with the results of STM studies of step dynamics at relatively low substrate temperatures [5, 6]. However, these models have not been compared with experiment at elevated temperatures, nor has the theory been compared with experiment in relation to the process of restoring the two-domain surface structure during annealing. This is due to the limitations of the STM method for studying surface processes occurring at high temperatures, over large surface areas, and over a long period of time. When using RHEED, these limitations are not so significant. However, since RHEED (unlike STM) does not allow direct observation of the surface on an atomic scale, it is necessary to specify functional relationships between the intensities of RHEED reflections and the characteristics of the surface relief.

In this work, the dynamics of monoatomic steps is studied based on the analysis of the RHEED reflex intensity variations under the assumption of a directly proportional relationship between the intensity of the reflection from the 1×2 superstructural domain and the A-terrace width [18]. The RHEED data were obtained during growth on Si(100) substrates with a miscut angle of 0.5° in the temperature range of 350–600 °C and at a growth rate of 0.07 monolayers (ML)/s. The restoring of the two-domain surface after growth interruption was studied on the same substrates in the same temperature range, as well as at a temperature of 600 °C on substrates with miscut angles of 0.3° and 0.1°. Using the models [12, 15], a numerical modeling of the step dynamics under the specified experimental conditions was performed. The time dependences of the A-terrace width during growth and annealing obtained by modeling are compared with the corresponding experimental dependences of the RHEED reflex intensity. An explanation is proposed for the experimentally obtained dependences of time, during which the steady-state value of the RHEED reflex intensity is reached, on temperature and the dependences of the surface recovery time during post-growth annealing on temperature and miscut angle.

2. Experimental

The growth and annealing were carried out in a Katun-S MBE setup equipped with an electron beam evaporator for silicon. The analytical part of the chamber consists of a quadrupole mass spectrometer, a quartz thickness gauge, and a 20 keV high-energy electron diffractometer. The Si(100) substrates were *n*-type with a resistivity of 5–10 Ohm cm and tilted from the (100) plane to the (111) plane strictly around the <110> axis by angles of 0.5°, 0.3°, and 0.1°. After the procedure of preparing the Si(100) surface in an ultrahigh vacuum chamber including removal of chemical oxide by annealing at 800 °C at a silicon atom flux of 10^{13} atoms/(cm^2·s) and growth of a 50 nm thick Si buffer layer, the substrate was annealed at 900 °C for 40 min (without a Si atom flux). Then, the substrate temperature was evenly decreased. In the substrate temperature range of 350–600 °C, the intensity of the reflection from the 1×2 superstructural domain was measured at a Si atom flux onto the substrate surface cor-

responding to a growth rate of 0.07 ML/s and a closed shutter of the Si atom source (during post-growth annealing). The change in the RHEED pattern was recorded in the azimuthal direction [100] using a video camera. The intensities of reflections located in the fractional-order Laue zone were analyzed.

3. RHEED intensity variations

In the initial stage of growth at low temperatures (350 and 400 °C), weak oscillations of the reflection intensity $I_{1\times2}(t)$ from the 1×2 superstructural domain are observed, which points to the 2D island nucleation growth mode or a transient growth mode due to the formation of islands and the movement of vicinal steps. Starting from 450 °C, the reflection intensity decreases monotonically with time down to some minimum (steady-state) value. This points to the step-flow growth mode and can be treated as a result of reducing the distance between the edges of the slow moving A-step and fast moving B-step until the width of the A-terrace reaches a certain minimum value. The decreasing dependences of the reflection intensity on time are shown in Fig. 1*a*, where $I_0 = I_{1\times2}(0)$ corresponds to the initial value of the intensity. The characteristic time of reaching the steady-state value of the reflection intensity was measured by constructing tangent lines at the beginning of the dependence $I_{1\times2}(t)/I_0$ and upon reaching a steady-state value of the intensity. The number of silicon monolayers n deposited until the steady-state is reached was determined as the product of this time and the growth rate. Figure 1*b* shows the temperature dependence of n. As can be seen, both this quantity and the steady-state value of the reflection intensity increase with increasing temperature. The same should be true for the minimum width of the A-terrace.

Figure 2*a* shows the time dependences of the intensity of reflection from the 1×2 superstructural domain in the temperature range of 450–600 °C after the shutter is closed or the flux of Si atoms is interrupted. According to the dependences in this figure, the intensity value tends to return to the initial level corresponding to the intensity of the RHEED reflection from the two-domain surface before growth. At 450 °C and, to a lesser extent, at 500 °C,

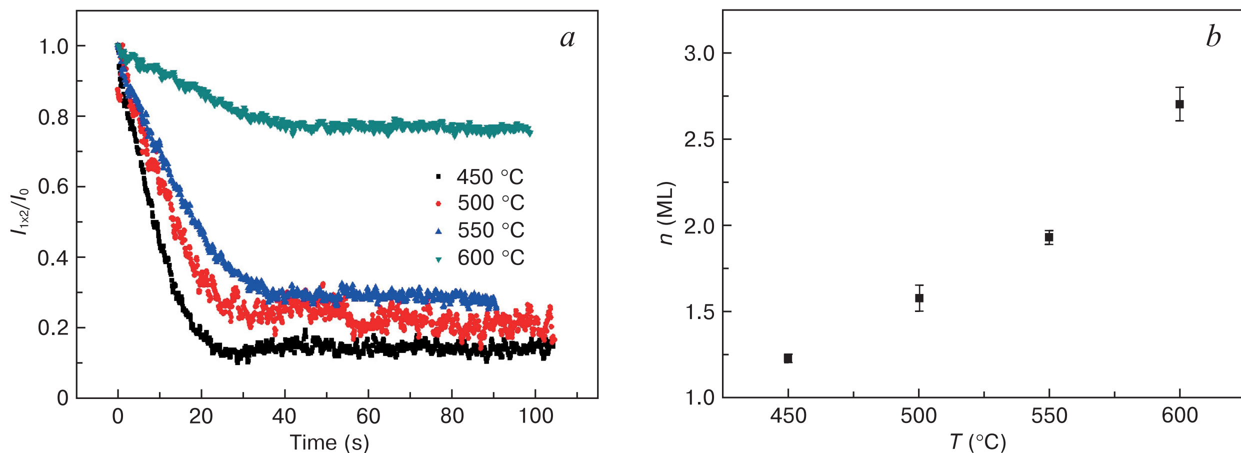

Figure 1. Results of the RHEED study of the dynamics of steps during growth: (*a*) RHEED reflex intensity variations for various substrate temperatures, (*b*) temperature dependence of the number of monolayers deposited until a steady-state value of the RHEED reflex intensity is reached

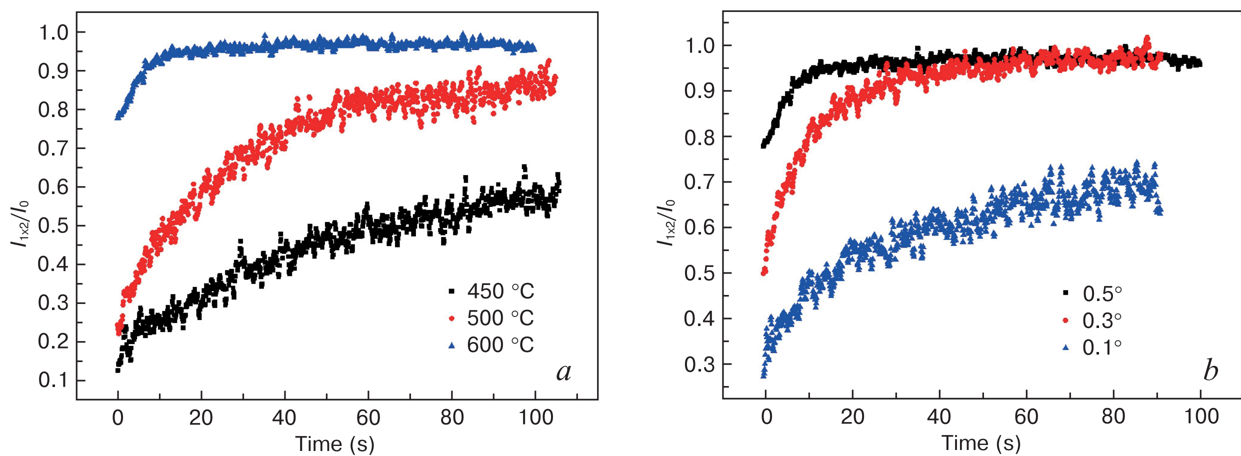

Figure 2. Time dependences of the $I_{1\times2}/I_0$ ratio after interruption of growth on a substrate with the miscut angel of 0.5° for various temperatures (*a*) and on substrates with various miscut angles at a temperature of 600 °C (*b*)

the ratio $I_{1\times2}/I_0$ does not reach a steady-state value, which does not allow us to correctly estimate the time during which recovery of the original surface occurs. However, it is quite obvious that with increasing temperature the surface recovery time decreases (Sakamoto et al. [8] also made mention of a decrease in the recovery time with increasing temperature, but the corresponding time dependences were not given in this work). Figure 2*b* shows the time dependences of the ratio $I_{1\times2}/I_0$ at 600 °C and various miscut angles. As can be seen, the recovery time decreases with the increasing miscut angle.

4. Modeling of the step dynamics

The dynamics of the steps was modeled by numerically integrating the equations of motion of the A- and B-steps:

$$\frac{dx_a}{dt} = V_a\left(L_a, L_b\right), \quad \frac{dx_b}{dt} = V_b\left(L_a, L_b\right), \qquad (1)$$

where $x_a(t)$ and $x_b(t)$ are the positions of the A- and B-steps along the axis perpendicular to the edges of the steps, $V_a(L_a, L_b)$ and $V_b(L_a, L_b)$ are the velocities of advance of the A- and B-steps, L_a and L_b are the widths of the A- and B-terraces. The expressions for the step velocities were obtained in [12, 15] using the solution of one-dimensional stationary continuity equations for the concentration of adatoms on the A- and B-terraces, taking into account the difference in the directions of fast diffusion on the terraces. When formulating the boundary conditions, it was assumed that the B-step is an ideal sink for adatoms and the concentration of adatoms near the edge of this step takes an equilibrium value. It was assumed also that the attachment of adatoms to the A-step from the upper and lower terraces requires overcoming additional (to the diffusion) energy barriers: the conventional and inverse Ehrlich–Schwoebel barriers [13, 14], respectively. In [15], it was also assumed that the migration of adatoms along the edge of the A-step is insignificant and, therefore, the A-step is permeable for adatoms. The effect of permeability of the B-step was not taken into account due to the high concentration of kinks at this step.

The expressions for the step velocities following from the model [15] are:

$$V_a = \left(\frac{L_a^2}{L_a + l_a} + \frac{L_b^2}{L_b + l_b}\right)\frac{R}{2\left(1 + M_p\right)} + \left(\frac{D_a}{L_a + l_a} + \frac{D_b}{L_b + l_b}\right)\frac{\tilde{n}_b - \tilde{n}_a}{1 + M_p};$$

$$V_b = \left[\frac{L_a l_a}{L_a + l_a} + \frac{L_b l_b}{L_b + l_b} + \left(L_a + L_b\right)\left(1 + M_p\right)\right] \times \frac{R}{2\left(1 + M_p\right)} - \left(\frac{D_a}{L_a + l_a} + \frac{D_b}{L_b + l_b}\right)\frac{\tilde{n}_b - \tilde{n}_a}{1 + M_p}, \qquad (2)$$

where R is the deposition flux of silicon atoms (in the absence of desorption, the flux R corresponds to the growth rate in monolayers per second), $D_a = a^2\nu\exp(-E_a/k_BT)$ and $D_b = a^2\nu\exp(-E_b/k_BT)$ are the surface diffusion coefficients of atoms on the A- and B-terraces, respectively (a is the interatomic distance on the surface, E_a and E_b are the activation energies, ν is the frequency factor, k_B is the Boltzmann constant), $l_a = a\exp(\Delta E_{ue}/k_BT)$ and $l_b = a\exp(\Delta E_{le}/k_BT)$ are the characteristic lengths associated with the possible presence of conventional (ΔE_{ue}) and inverse (ΔE_{le}) Ehrlich–Schwoebel barriers for the attachment of adatoms to the A-step from the A- and B-terraces, respectively, $\tilde{n}_a$ and $\tilde{n}_b$ are the relative concentrations of adatoms in equilibrium with the A- and B-steps, respectively. The quantity

$$M_p = \frac{\left(1 - \theta_k\right) l_a l_b}{\theta_k\left(L_a + l_a\right)\left(L_b + l_b\right)}\left(1 + \frac{D_a L_b + D_b L_a}{D_a l_b + D_b l_a}\right),$$

where θ_k is the relative concentration of kinks, takes into account the effect of permeability of the A-step. If $\theta_k = 1$, then the A-step is impermeable and expressions (2) are reduced to the corresponding expressions for the step velocities obtained in [12].

In the given expressions, L_a, L_b, $\tilde{n}_a$ and $\tilde{n}_b$ depend on time. It was assumed that at the initial moment of time all steps are at the same distance from each other $L_a(0) = L_b(0) = L_0$, which is determined by the miscut angle. Assuming for the initial position of the steps $x_a(0) = L_0$ and $x_b(0) = 0$, one can write $L_a(t) = x_a(t) - x_b(t)$ and $L_b(t) = 2L_0 + x_b(t) - x_a(t)$. For the difference in the equilibrium concentrations of adatoms, the expression obtained in [12] was used:

$$\tilde{n}_b(t) - \tilde{n}_a(t) = 2\tilde{n}\sinh\left\{\frac{\pi\alpha a^2}{2L_0 k_B T} \times \cot\left[\frac{\pi\left(x_a(t) - x_b(t)\right)}{2L_0}\right]\right\},$$

where α is the constant of elastic repulsion of the steps and $\tilde{n} = \exp(-\Delta E/k_BT)$ is the equilibrium concentration of adatoms in the case of equidistant steps (i.e., at $L_a = L_b = L_0$). Here ΔE is the formation energy of an adatom [12]. Thus, Eqs (1) represent a system of nonlinear differential equations with respect to $x_a(t)$ and $x_b(t)$, which allows a numerical solution with an appropriate choice of model parameters.

The numerical integration of Eqs (1) was performed using the values of the parameters characteristic for the Si(100) surface: $a = 0.384$ nm, $\alpha = 2.36\cdot10^{-2}$ eV/nm [19], and $\nu = 10^{13}$ s^{-1}. In accordance with the miscut angle $\theta = 0.5°$, the initial distance between the steps L_0 was assumed to be 16 nm. The surface diffusion activation energies were taken to be $E_a = 1.19$ eV and $E_b = 0.65$ eV [20]. In the case of a permeable A-step, the concentration of kinks was calculated using the formula [21]

$$\theta_k = \frac{1}{1 + 0.5\exp\left(\frac{\varepsilon_k}{k_B T}\right)},$$

where the kink formation energy was assumed to be 0.2 eV [22]. Two sets of parameters were used for each type of A-step. For impermeable ($\theta_k = 1$) A-steps: ΔE_{ue} = 0.3 eV, ΔE_{le} = 0.4 eV, ΔE = 0.8 eV (set 1) and ΔE_{ue} = 0.1 eV, ΔE_{le} = 0.3 eV, ΔE = 1 eV (set 2) were assumed. For permeable ($\theta_k < 1$) A-steps, in accordance with the results of ab initio calculations [23], the conventional Ehrlich–Schwoebel ΔE_{ue} was set zero, whereas ΔE_{le} = 0.2 eV [24], ΔE = 1 eV (set 1) and ΔE_{le} = 0.05 eV, ΔE = 1 eV (set 2) were assumed. The values of parameter set 1 correspond to those used in [10]. Numerical modeling based on the models [12] and [15] gave similar results. Therefore, only the results of modeling based on the permeable A-step model [15] are presented below.

5. Results of modeling

Modeling of the step dynamics on the surface with miscut angle of 0.5° at a growth rate of 0.07 ML/s demonstrates that the width of the A-terrace decreases as the growth time increases and tends asymptotically toward a stationary value $L_{a,st}$, which increases with increasing temperature. The corresponding dependences are shown in Fig. 3*a* by solid lines when using parameter set 1 and by dashed lines for parameter set 2. According to [12], the increase in $L_{a,st}$ with increasing temperature is associated with an increase in the exchange flux of atoms between the A- and B-steps, caused by the elastic interaction between the steps. Despite the similarity of the dependences in Fig. 3*a* with the RHEED reflex intensity variations in Fig. 1*a*, there is a significant difference between the theoretical predictions and experimental data. In contrast to the experiment, the modeling demonstrates a non-monotonic dependence $n(T)$: a very weak increase of n at low T and a decrease at high T (Fig. 3*b*). It should be noted that the $n \approx 0.5$ ML value obtained using parameter set 1 agrees with the results of observing formation of bilayer steps using STM [5]. Reducing the barrier for adatom attachment to the A-step in the case of using parameter set 2 leads to an increase of n up to 1.2 ML, which at T = 450 °C is consistent with the experimental results shown in Fig. 1*b*. This is explained by a decrease in the difference in the velocities of the A- and B-steps due to a decrease in the barrier ΔE_{el} and, accordingly, an increase in the intensity of adatom incorporation into the A-step. However, with an increase in temperature, the values of n become significantly smaller than the experimental ones. At the same time, starting from T = 550 °C, the value of n decreases with increasing temperature. Within the framework of models [12, 15], this is explained by an increase in the steady-state width of the A-terrace due to an increase in the exchange flux of atoms between the A- and B-steps preventing the formation of biatomic steps (as a consequence, the distance, that the steps travel until the minimum width of the A-terrace is achieved, decreases).

Figure 4*a* shows the time dependences of the A-terrace width (related to the initial terrace width L_0) on the surface with a miscut angle of 0.5° at different annealing temperatures. The initial values of the L_a/L_0 ratios correspond to the initial values of the ratios $I_{1\times2}/I_0$ of the RHEED reflection intensities in Fig. 2*a*. In accordance with the experimental results shown in Fig. 2*a*, the modeling demonstrates an increase in the A-terrace width (recovering of the original surface) during annealing. This process accelerates as the substrate temperature increases which is explained by the increase in the exchange flux of atoms between the A- and B-steps due to increasing mobility of adatoms and increasing frequency of detachment of atoms from the B-steps. Recovering of the original surface also accelerates with an increase in the miscut angle θ (Fig. 4*b*). This is due to the fact that with the increasing θ the average width of the terraces decreases and, consequently, the probability that an atom detached from a B-step will reach an A-step before returning back

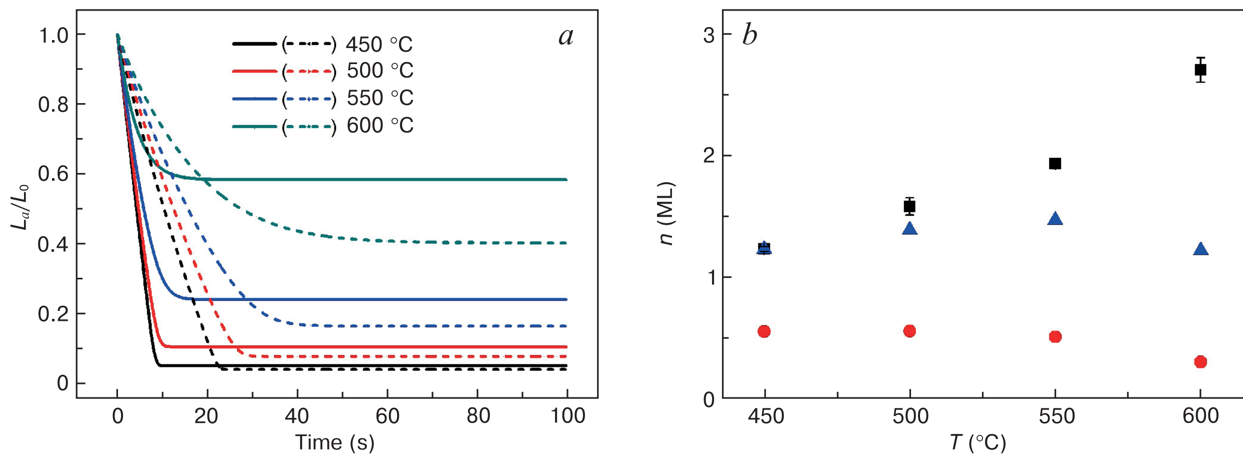

Figure 3. Results of modeling the motion of A- and B-steps during growth at different substrate temperatures: (*a*) time dependences of the A-terrace width (solid and dotted lines refer to different sets of model parameters, see text of the article), (*b*) the number of Si monolayers deposited until the steady-state value of the A-terrace width is reached (squares are the experimental values in Fig. 2*b*, circles and squares are the values obtained using modeling with parameters corresponding to the solid and dotted lines in Fig. 3*a*, respectively)

increases. Thus, the magnitude of the exchange flux of atoms between the A- and B-steps increases.

It should be noted that the dependences in Fig. 4 obtained using parameter set 1 are significantly closer to the time dependences of the RHEED reflection intensity in Fig. 2 than the dependences obtained using set 2. Thus, an attempt to improve the fit of the model to experimental data on step dynamics during growth results in a worse fit to experimental data on the step dynamics during annealing. The performed extensive modeling showed that no reasonable choice of parameters exists that enable achieving quantitative agreement between the models [12, 15] and the experimental results in a wide temperature range.

6. Discussion

The obtained time dependences of the RHEED reflection intensity $I_{1\times2}(t)$ demonstrate a decrease of $I_{1\times2}(t)$ during growth in the temperature range of 450–600 °C down to a steady-state value $I_{1\times2,st}$ and an increase of $I_{1\times2}(t)$ after growth interruption (during annealing) up to the steady-state value close to the value of the RHEED reflection intensity from the initial two-domain surface. The steady-state intensity $I_{1\times2,st}$ increases with increasing temperature whereas the characteristic time of recovery of the initial surface during annealing decreases with increasing temperature. These results are in qualitative agreement with predictions of the models [12, 15], if we assume that the intensity of the reflection from the 1×2 superstructural domain is directly proportional to the width of the A-terrace. However, the available models fail to explain the experimentally obtained increasing dependence on temperature of the number of monolayers deposited until the steady-state value of the reflection intensity is reached during growth.

It is worth noting that in [6], the A- and B-step dynamics was studied using STM at a fixed temperature and at two different values of the Si deposition flux (the Si growth rate R). According to [6], an increase in R leads to a significantly sharper increase of the width of the B-terraces with the increasing surface coverage (the product of R and the deposition time) at the initial stage of growth. This result also cannot be explained within the framework of the models [12, 15], since in these models the step velocities depend linearly on R (see Eq. 2) and, therefore, the rate of change of the terrace width with the increasing surface coverage should not depend on R.

The reason for such discrepancies may be a simplified description of the incorporation of adatoms into steps, which does not take into account the structural features of the Si(100)-2×1 surface. As is known, the elemental building unit on this surface is two dimers in a kink on a step [2, 25]. The formation of dimer rows or dimers in kinks includes elementary processes of adatom attachment, detachment of a single atom from a dimer, and dimer dissociation. As a result of the dissociation, one atom leaves the kink and the other remains in the position of a single atom in the kink [11]. In the general case, the expression for the rate of kink motion (lengthening of the dimer row) has a form of a nonlinear combination of elementary frequencies of attachment, detachment, and dissociation.

Modeling the dynamics of steps that takes into account the above-mentioned peculiarities of formation of building units in the kinks requires solving the continuity equations with nonlinear boundary conditions at the edges of the A- and B-steps, which is a separate complex problem. However, one can point out a significant difference in the kinetics of adatom incorporation into steps in the cases of low and high temperatures (small and large fluxes of deposited atoms). At low frequencies of adatom detachment and/or high frequencies of adatom attachment (low temperature and/or large value of the deposition flux), the probability of detachment of a single atom before the next atom arrives at the kink is small and a single atom in the kink can be considered as incorporated in the crystal (with a high probability, a dimer is formed). The influence of the peculiarities of adatom incorporation in the

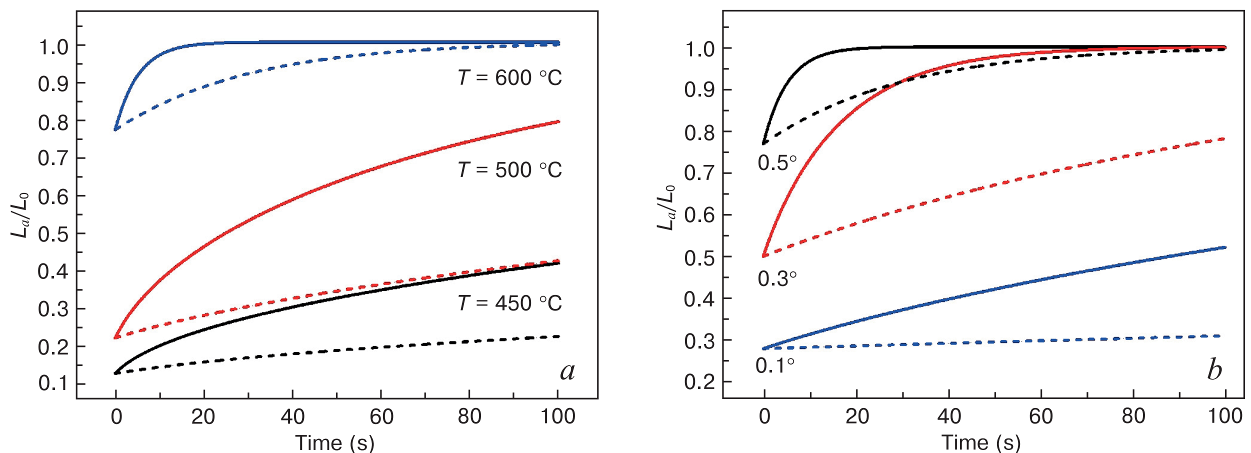

Figure 4. Results of modeling the recovering of the original surface after growth interruption (during annealing): (*a*) time dependences of the A-terrace width on the surface with the miscut angle of 0.5° for various annealing temperatures, (*b*) time dependences of the A-terrace width on the surfaces with various miscut angles at an annealing temperature of 600 °C

kinks is insignificant in this case and the expressions obtained in [12, 15] for the step velocities can be used in the modeling of step dynamics. However, at high frequencies of adatom detachment and/or low frequencies of adatom attachment, the formation of building units is limited by the meeting of two adatoms at the kinks. In this case, an adatom entering a kink from one of the terraces has the opportunity to move to the neighboring terrace. The formulation of boundary conditions for the continuity equations used in [12, 15] seems incorrect in this case, since the steps are permeable for adatoms regardless of the concentration of kinks. In particular, the B-step can no longer be considered as an ideal sink for adatoms. This should result in a significant decrease in the difference in the velocities of A- and B-steps and, consequently, an increase in the number of Si monolayers deposited until the minimum value of the A-terrace width is achieved might be expected.

7. Conclusions

The RHEED method is used to study the dynamics of monoatomic steps on the reconstructed 1×2 Si(100) vicinal surface during MBE growth and annealing in a wide range of substrate temperatures. The obtained time dependences of the RHEED reflection intensity from the 1×2 superstructural domain demonstrate a decrease in the intensity during growth to a steady-state value. When the growth is interrupted (during annealing), the RHEED reflection intensity increases tending to the intensity value from the two-domain surface before growth. The obtained experimental dependences are in qualitative agreement with the time dependences of the A-terrace width obtained by numerical modeling of the step dynamics based on the available models of the A- and B-step motion on the Si(100) surface. A comparison of the modeling results with the experiment makes it possible to explain the experimentally observed increase in the steady-state value of the RHEED intensity with increasing temperature as well as a decrease in the surface recovery time during annealing with increasing temperature and the miscut angle. However, the modeling fails to reproduce the experimentally obtained monotonically increasing temperature dependence of the number of monolayers deposited until a steady-state value of the RHEED reflex intensity is reached. This may be due to the peculiarities of the formation of building units in the kinks on the reconstructed Si(100) surface that are not taken into account in the available models.

References

1. Dabrowski J., Mussig H.-J. Silicon surfaces and formation of interfaces: basic science in the industrial world. World Scientific; 2000. 576 p. https://doi.org/10.1142/3615
2. Markov I.V. Crystal growth for beginners: Fundamentals of nucleation, crystal growth and epitaxy. 2nd ed. Singapore: World Scientific; 2003. 564 p. https://doi.org/10.1142/5172
3. Bolkhovityanov Yu.B., Pchelyakov O.P. GaAs epitaxy on Si substrates: modern status of research and engineering. *Physics-Uspekhi*. 2008; 51(5): 437–456. http://doi.org/10.1070/PU2008v051n05ABEH006529
4. Alerhand O.L., Vanderbilt D., Meade R.D., Joannopoulos J.D. Spontaneous formation of stress domains on crystal surfaces. *Physical Review Letters*. 1988; 61(17): 1973–1976. https://doi.org/10.1103/PhysRevLett.61.1973
5. Hoeven A.J., Lenssinck J.M., Dijkkamp D., van Loenen E.J., Dieleman J. Scanning-tunneling-microscopy study of single-domain Si(001) surfaces grown by molecular-beam epitaxy. *Physical Review Letters*. 1989; 63(17): 1830–1832. https://doi.org/10.1103/PhysRevLett.63.1830
6. Voigtländer B., Weber T., Šmilauer P., Wolf D.E. Transition from Island growth to step-flow growth for Si/Si(100) epitaxy. *Physical Review Letters*. 1997; 78(11): 2164–2167. https://doi.org/10.1103/PhysRevLett.78.2164
7. Aizaki N., Tatsumi T. In situ RHEED observation of selective diminution at Si(001)-2×1 superlattice spots during MBE. *Surface Science*. 1986; 174(1-3): 658–665. https://doi.org/10.1016/0039-6028(86)90488-7
8. Sakamoto K., Sakamoto T., Miki K., Nagao S. Observation of Si(001) vicinal surfaces on RHEED. *Journal of The Electrochemical Society*. 1989;136(9):2705–2709.
9. Yesin M.Yu., Deryabin A.S., Kolesnikov A.V., Nikiforov A.I. Study of Si(100) surface step convergence kinetics. *Physics of the Solid State*. 2023; 65(2): 167–173. https://https://doi.org/10.21883/PSS.2023.02.55397.476
10. Hervieu Yu.Yu., Yesin M.Yu., Deryabin A.S., Kolesnikov A.V., Nikiforov A.I. Pairing of monoatomic steps on the Si(100) surface: experiment and modeling. *Izvestiya vuzov. Fizika*. 2023; 66(4(785)): 85–92. (In Russ.). https://doi.org/10.17223/00213411/66/4/10
11. Stoyanov S. Formation of bilayer steps during growth and evaporation of Si(001) vicinal surfaces. *Europhysics Letters*. 1990; 11(4): 361–366. https://doi.org/10.1209/0295-5075/11/4/012
12. Hong W., Zhang Z., Suo Z. Interplay between elastic interactions and kinetic processes in stepped Si(001) homoepitaxy. *Physical Review B*. 2006; 74(23): 235318. https://doi.org/10.1103/PhysRevB.74.235318
13. Ehrlich G., Hudda F.G. Atomic view of surface self-diffusion: tungsten on tungsten. *The Journal of Chemical Physics*. 1996; 44(3): 1039–1049. https://doi.org/10.1063/1.1726787
14. Schwoebel R.L., Chipsey E.J. Step motion on crystal surface. *Journal of Applied Physics*. 1966; 37(10): 3682–3686. https://doi.org/10.1063/1.1707904
15. Hervieu Yu.Yu. Formation of double steps on Si(100): effect of permeability of A-steps. *Russian Physics Journal*. 2020; 63(6): 901–906. https://doi.org/10.1007/s11182-020-02116-1

16. Tanaka S., Bartelt N.C., Umbach C.C., Tromp R.M., Blakely J.M. Step permeability and the relaxation of biperiodic gratings on Si(001). *Physical Review Letters*. 1997; 78(17): 3342–3345. https://doi.org/10.1103/PhysRevLett.78.3342
17. Filimonov S.N., Hervieu Yu.Yu. Terrace-edge-kink model of atomic processes at the permeable steps. *Surface Science*. 2004; 553(1-3): 133–144. https://doi.org/10.1016/j.susc.2004.01.047
18. Vasev A.V., Putyato M.A., Preobrazhenskii V.V. Some geometrical aspects of diffracted waves formation on a reconstructed crystal face at RHEED. *Surface Science*. 2018; 677: 306–315. https://doi.org/10.1016/j.susc.2018.08.005
19. Poon T.W., Yip S., Ho P.S., Abraham F.F. Ledge interactions and stress relaxations on Si(001) stepped surfaces. *Physical Review B*. 1992; 45(7): 3521–3531. https://doi.org/10.1103/PhysRevB.45.3521
20. Shu D.J., Liu F., Gong X.G. Simple generic method for predicting the effect of strain on surface diffusion. *Physical Review B*. 2001; 64(24): 245410. https://doi.org/10.1103/PhysRevB.64.245410
21. Burton W.K., Cabrera N., Frank F. The growth of crystals and the equilibrium structure of their surfaces. *Philosophical Transactions of the Royal Society A*. 1951; 243(866): 299–358. https://doi.org/10.1098/rsta.1951.0006
22. Zandvliet H.J.W. Energetics of Si(001). *Reviews of Modern Physics*. 2000; 72(2): 593–602. https://doi.org/10.1103/RevModPhys.72.593
23. Zhang Q.-M., Roland C., Bogusławski P., Bernholc J. Ab initio studies of the diffusion barriers at single-height Si(100) steps. *Physical Review Letters*. 1995; 75(1): 101–104. https://doi.org/10.1103/PhysRevLett.75.101
24. Wang J., Drabold D.A., Rockett A. Binding and diffusion of a Si adatom around the type A step on Si(001) c(4×2). *Applied Physics Letters*. 1995; 66(15): 1954–1956. https://doi.org/10.1063/1.113288
25. Swartzentruber B.S., Mo Y.-W., Kariotis R., Lagally M.G., Webb M.B. Direct determination of step and kink energies on vicinal Si(001). *Physical Review Letters*. 1990; 65(15): 1913–1916. https://doi.org/10.1103/PhysRevLett.65.1913